

## Research Article

# Study on Gas Enrichment Mechanism of Coal Seam Influenced by Vertical Stress on Mountainous Region Condition

Xiaojie Yang,<sup>1,2</sup> Ruifeng Huang<sup>1,2</sup>, Shuhua Sun,<sup>3</sup> Chaowen Hu<sup>4</sup>, Bo Cheng,<sup>5</sup> Jianning Liu,<sup>1,2</sup> and Feng Zhang<sup>5</sup>

<sup>1</sup>State Key Laboratory for Geomechanics & Deep Underground Engineering, China University of Mining & Technology, Beijing 10083, China

<sup>2</sup>School of Civil and Architecture Engineering, China University of Mining and Technology, Beijing 100083, China

<sup>3</sup>Shandong Energy Yanzhou Coal Mining Company Limited, Jining, Shandong 273500, China

<sup>4</sup>Transportation Institute, Inner Mongolia University, Hohhot, Inner Mongolia 010070, China

<sup>5</sup>China Coal Technology Engineering Group Chongqing Research Institute, Chongqing 400037, China

Correspondence should be addressed to Ruifeng Huang; [hrcumt@163.com](mailto:hrcumt@163.com)

Received 22 September 2020; Revised 20 November 2020; Accepted 8 December 2020; Published 21 December 2020

Academic Editor: chen miao

Copyright © 2020 Xiaojie Yang et al. This is an open access article distributed under the Creative Commons Attribution License, which permits unrestricted use, distribution, and reproduction in any medium, provided the original work is properly cited.

The controlling effect of vertical stress of mountainous region on gas occurrence of the coal seam below it has always been ignored. In order to clearly express its influence mechanism, the change laws of depth, stress, and permeability of coal seam pressurised by the overlying mountain were studied based on the Winkler elastic foundation beam theory and seepage theory in the paper. At the same time, the enrichment mechanism of the coal seam pressurised by the overlying mountain was analyzed. The results showed the following: (1) There was a significantly strong correlation between the stress, permeability change rule of the coal seam, burial depth, and surface elevation under such condition. (2) Under the action of the vertical pressure of the mountain, the stress and permeability distribution of the coal seam showed significant nonlinear characteristics. The stress was the greatest under the peak, and the permeability was the smallest. (3) The initial gas content value was controlled by the permeability and the stress of the coal seam in the situation. Moreover, the field practice showed that under the action of vertical pressure of the mountain, the evaluation law of gas content was coupling with the surface elevation of the overlying mountain. In addition, the gas emission change law during the excavation of the driving face also showed the same characteristics. The results might be of great significance for the development and utilization of coal-bed gas and the safe exploitation of coal resources.

## 1. Introduction

The coal reservoir permeability affected by pressure, pores, cracks, and other factors is of great significance to coal-bed methane occurrence, gas development and utilization, and safe mining of coal resources. Recently, there has been growing interest in the mechanical relationship between permeability and stress state in mining engineering. It is well known that permeability is an important parameter characterizing the flow capacity of gas in coal mass. Coal porosity and permeability are key petrophysical parameters, pivotal in facilitating coal-bed methane extraction and CO<sub>2</sub> sequestration [1]. The gas flow capacity of coal seam increases

with the rise of permeability. Some researchers have found that the coal seam permeability is closely related to its stress state [2, 3]. In the elastic deformation stage, permeability generally reduces with increasing pressure [4–6], which plays a restrictive role on the flow of gas. In the southern margin of the Junggar Basin, researchers found that permeability gradually decreases from the reservoir top to the base due to depth-increasing stress while gas content gradually increases due to permeability [7]. Meanwhile, the permeability often increases with decrease in pressure [8–11]. The permeability-strain curve of coal has a similar change rule for the stress-strain curve. The cracks in surrounding rock are also closed by increasing pressure,

resulting in the reduction in rock permeability [5, 12]. Generally, burial depth of the coal seam can directly control its stress, which indirectly controls the permeability for predictable reasons. To further clarify the relationship between the three, more studies have been published by scholars in the field of rock mechanics. For ground stress increases with the increase in burial depth, the permeability of the coal seam decreases gradually [13–15] and the gas content of the coal body increases as burial depth of coal seam increases [16–18]. The influence mechanism of burial depth on gas content can be expressed as follows according to the above investigations: the permeability of the coal seam is controlled directly by the stress associated with burial depth, which has strong correlation with gas flow. It implies that the high ground stress and low permeability might induce gas enrichment of the coal seam in complex coal-forming and geology movement process. The more detailed logical relationships among burial depth, stress, permeability, and gas enrichment are shown in Figure 1.

Figure 1 implies that gas flow might be affected by the permeability at a certain place. The result of [19] indicates that the permeability also affects the gas flow, with the larger permeability regions having the higher daily production. On this basis, we can indirectly evaluate the permeability via gas flow laws.

On condition of mountainous topography, the surface elevation often changes dramatically, causing huge changes in the burial depth of the coal seam. Thus, the burial depth, stress, and permeability of the coal seam change simultaneously, resulting in the great difference in gas reservation on the identical coal seam. It will be reflected on gas content of the coal seam and the amount of gas emission in the process of coal roadway excavation. At present, there is less research on this important phenomenon, which needs to be analyzed and studied.

The aim of the investigation here was to analyze the inner mechanism of mountainous topography to gas enrichment. The Winkler elastic foundation beam theory was used to establish the mechanical model so as to analyze the stress and permeability change rules of the coal seam pressurised by the overlying mountain. Also, we carried out several sets of case experiments to test the validity of the research results. This pioneer work might contribute to our present understanding of gas enrichment mechanism and is of great significance for the development and utilization of coal-bed gas and the safe exploitation of coal resources.

## 2. Mechanical Model

**2.1. Establishment of the Mechanical Model.** In underground mines, the thickness of the coal seam is extremely thin compared with overburden strata and thus it can be simplified as a beam. To study the characteristics of the coal seam pressurised by overlying mountains, the coal seam was simplified to an infinite long beam and a mechanical model under the action of a single mountain was established. The typical model is shown in Figure 2.

Some hypotheses should be proposed as follows: (1) The weight of overlying rock except for the part of the mountain

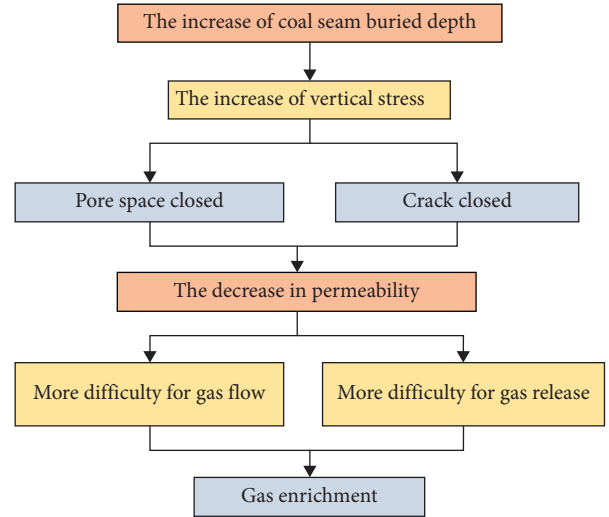


FIGURE 1: The relationship between burial depth, stress, permeability, and gas enrichment.

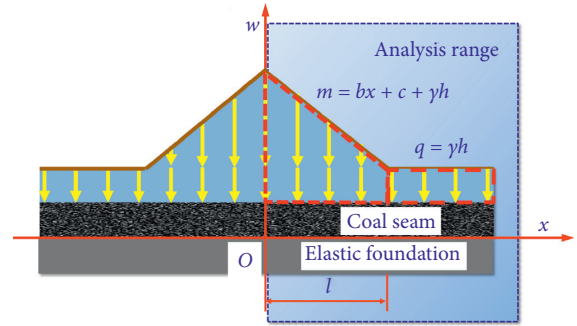


FIGURE 2: A typical mechanical model of the coal seam pressurised by a mountain.

can be simplified as a uniform load  $q = \gamma h$ , where  $\gamma$  is the rock mass bulk and  $h$  is the distance from the coal seam to the surface. (2) The effect of the mountain on the coal seam is equivalent to a trapezoidal-distributed load  $m = bx + c + \gamma h$ , wherein  $b$  is the slope and the  $c + \gamma h$  is the vertical pressure of the overlying rock layers and the peak of the mountain at the  $O$  point. (3) Tectonic stress is not considered here.

**2.2. Theoretical Solution of the Mechanical Model.** The width of the beam can be assumed as 1, and the establishment of a rectangular coordinate system is shown in Figure 2. According to the Winkler elastic foundation beam theory, the model deflection curve can be expressed with [20, 21]

$$w = e^{ax} (A \cos ax + B \sin ax) + e^{-ax} (C \cos ax + D \sin ax) + w_0(x), \quad (1)$$

where  $e$  is the nature base;  $a$  is the characteristic coefficient; in  $a^4 = K/4EI$ ,  $K$  is the foundation stiffness; the  $EI$  is the flexural section stiffness;  $A$ ,  $B$ ,  $C$ , and  $D$  are the undetermined coefficients; and  $w_0(x)$  represents the special solution of the equation.

The model is axisymmetric, and only the analysis range of the right part of the  $w$  axis of the model was studied, and the pressure on the coal seam can be represented by segmented functions as follows:

$$\begin{cases} m = bx + c + \gamma h, & 0 \leq x < lm, \\ q = \gamma h, & x \geq l. \end{cases} \quad (2)$$

Any microsegment  $dx$  was taken; based on the mechanical equilibrium relation, the deflection differential equation of the model can be expressed with

$$w^{(4)} + 4a^{(4)}w = \frac{b}{EI}x + \frac{c + \gamma h}{EI}. \quad (3)$$

Equation (3) is a four-order constant-coefficient nonhomogeneous linear differential equation, the solution of which is composed of the common solution to the homogeneous equation and the special solutions to the nonhomogeneous equation.

There are two nonhomogeneous items in equation (3), which can be written as  $w_{01}(x)$  and  $w_{02}(x)$ . The first special solution  $w_{01}(x)$  and the second special solution  $w_{02}(x)$  to the right side of equation 3 can be solved. Then, use the superposition principle to obtain  $w_0(x)$ .

The expressions of  $w_{01}(x)$  and  $w_{02}(x)$  were obtained by mathematical knowledge as follows:

$$\begin{cases} w_{01}(x) = \frac{c + \gamma h}{K}, \\ w_{02}(x) = \frac{b}{K}x. \end{cases} \quad (4)$$

Expression  $w_0(x)$  was the sum of  $w_{01}(x)$  and  $w_{02}(x)$ :

$$w_0(x) = \frac{bx + c}{K} + \frac{\gamma h}{K}. \quad (5)$$

Therefore, the deflection equation of the coal seam can be expressed as

$$w = e^{ax} (A \cos ax + B \sin ax) + e^{-ax} (C \cos ax + D \sin ax) + \frac{bx + c}{K} + \frac{\gamma h}{K}. \quad (6)$$

According to the Winkler elastic foundation beam theory, nominal stress on the coal seams can be expressed as

$$\sigma = Kw. \quad (7)$$

Equation (8) can be obtained by inserting equation (6) into equation (7):

$$\sigma = K[e^{ax} (A \cos ax + B \sin ax) + e^{-ax} (C \cos ax + D \sin ax)] + bx + c + \gamma h. \quad (8)$$

(1) When  $0 \leq x < l$ , the coal seam is only subject to the trapezoidal distribution load. It can be known by natural boundary conditions and continuous deformation conditions:  $\theta|_{x=0} = 0$ ,  $EI(d^3w_1/dx^3)|_{x=0} = 0$ ,  $w|_{x=l} = \gamma h/K$ , and  $\theta|_{x=l} = 0$ . Moreover,

the expressions of  $A_1$ ,  $B_1$ ,  $C_1$ , and  $D_1$  can be obtained by using it:

$$\begin{cases} A_1 = D_1 \frac{(e^{al} - e^{-al})\sin al}{(e^{al} + e^{-al})\cos al} + \frac{b(e^{al}\sin al - e^{-al}\cos al)}{2aK(e^{al} + e^{-al})\cos al}, \\ B_1 = \frac{b}{2aK} - D_1, \\ C_1 = A_1 + \frac{b}{2aK}, \\ D_1 = \frac{b[(e^{al}\sin al + e^{al}\cos al + e^{-al}\cos al + e^{-al}\sin al - 2a)(e^{al} + e^{-al})\cos al - (e^{al}\sin al - e^{-al}\cos al)(e^{al}\cos al - e^{al}\sin al - e^{-al}\cos al - e^{-al}\sin al)]}{2aK[(e^{al} - e^{-al})(e^{al}\cos al - e^{al}\sin al - e^{-al}\cos al - e^{-al}\sin al)\sin al - (e^{al}\sin al + e^{al}\cos al - e^{-al}\cos al + e^{-al}\sin al)(e^{al} + e^{-al})\cos al]}. \end{cases} \quad (9)$$

The nominal stress equation of the infinite long beam when  $0 \leq x < l$  can be obtained conveniently by inserting equation (9) into equation (8).

- (2) When  $x \geq l$ ,  $bx + c = 0$  in the third item in equation (6), and the following can be known from natural boundary conditions and continuity conditions:  $w_2|_{x \rightarrow +\infty} = \gamma h/K$  and  $w_2|_{x \rightarrow l} = \gamma h/K$ . Then, the expressions of  $A_2 = B_2 = 0$  and  $C_2 = D_2 = 0$  can be

obtained by using it. Equation (10) can be obtained by inserting it into equation (8):

$$\sigma_2 = \gamma h. \quad (10)$$

Then, the nominal stress of the coal seam can be expressed with the segmented functions as follows:

$$\begin{cases} \sigma_1 = K[e^{ax}(A_1 \cos ax + B_1 \sin ax) + e^{-ax}(C_1 \cos ax + D_1 \sin ax)] + bx + c + \gamma h, & 0 \leq x < l, \\ \sigma_2 = \gamma h, & x \geq l. \end{cases} \quad (11)$$

From equations (9) and (11), we can see the influence factors of nominal stress considering vertical pressure of the mountain are different on different locations of the coal seam. (1) In the influence area of the trapezoidal load, the nominal stress of the coal seam is mainly comprehensive affected by slope  $b$ , flexural section stiffness  $EI$ , foundation stiffness  $K$ , and vertical pressure  $c + \gamma h$  at point O. (2) In other regions, the main influence factor of nominal stress is the uniform load  $\gamma h$ .

The study [22] showed that the nominal stress  $\sigma$  was related to gas pressure  $p$ , effective stress  $\sigma^T$ , and porosity  $\phi$ :

$$\sigma^T = \frac{\sigma - p\phi}{1 - \phi}. \quad (12)$$

Considering the compression deformation characteristics of the solid skeleton of the porous media, the porosity state equation can be introduced:

$$\phi = \phi_0 [1 + c_\phi (p - p_0)], \quad (13)$$

where  $\phi_0$  is the initial porosity, %;  $c_\phi$  is the pore compressibility,  $10^{-3} \text{MPa}^{-1}$ ;  $p$  is the gas pressure, MPa; and  $p_0$  is the initial gas pressure, MPa.

Based on the experimental study [23], permeability is generally exponentially related to effective stress, which can be expressed as follows:

$$k = ek_0 \exp(d\sigma^T), \quad (14)$$

where  $k$  is the permeability,  $\text{m}^2$ ;  $k_0$  is the initial permeability,  $\text{m}^2$ ; and  $e$  and  $d$  are constants.

Let  $u = ek_0 \exp(d)$ ; the following equation can be obtained according to Equations (12)–(14):

$$\frac{k}{u} = \exp \left\{ \frac{\sigma - p\phi_0 [1 + c_\phi (p - p_0)]}{1 - \phi_0 [1 + c_\phi (p - p_0)]} \right\}. \quad (15)$$

Equation (15) is an equation containing nominal stress, gas pressure, and permeability. Compared with other research results, equation (15) eliminates the influence of uncertain effective stress and directly adopts nominal stress as a variable. At the same time, the influence mechanism of effective stress and the shrinkage effect of the porous media

matrix on permeability are also considered in the equation, which has a great significance to practical value.

The equation of coal seam permeability based on Figure 2 can be obtained by comprehensive equations (9), (11), and (15). Given the length of the paper, the formula is omitted in the section. Those researchers who are interested in that can obtain the formula easily by taking equation (9) and equation (15) into equation (11). It is easy to see that the formula contains stress controlled by the burial depth and permeability affected by porosity of the coal seam. The relationships among burial depth, stress, and permeability will be studied in the following section.

### 3. Stress and Permeability Change Rules of the Coal Seam on Mountainous Region Condition

**3.1. Stress Characteristics of the Coal Seam Pressurised by the Overlying Mountain.** According to the above mechanical analysis, the stress characteristics of the mountain pressurised by the coal seam would be studied by an example analysis method. Coal seam thickness was taken as 8 m, and its elastic modulus  $E = 3.38 \text{GPa}$ ; thus,  $EI = 144.21 \times 10^9 \text{N}\cdot\text{m}^2$ . The stiffness  $K$  of coal seam foundation was  $0.25\text{--}1.00 \text{GPa}$  [24], where  $K = 0.5 \text{GPa}$  was taken in here and  $l = 50 \text{m}$ , the  $\gamma h = 5, 10, 15 \text{MPa}$ ,  $c = 7, 10, 15 \text{MPa}$ , and  $b = -0.1$  were taken for the convenience to research.

Based on the above values and equation (11), the stress characteristics of the coal seam were studied as follows. Figures 3 and 4 represent the nominal stress curves of coal seams with a different uniform load  $\gamma h$  and parameter  $c$ , respectively.

The following can be seen from Figures 3 and 4: (1) On condition of a vertical pressure of the mountain, the nominal stress of the coal seam is characterized by significant non-linearity, which directly leads to the uneven stress of the coal seam at the same floor elevation. (2) Under the condition of equal uniform load  $\gamma h$ , with the increase of the value of parameter  $c$ , the nominal stress of the coal seam is increasing meanwhile. In addition, the larger the value of  $c$  is, the more obvious the degree of nonlinearity is. (3) Under the condition of the same value of parameter  $c$ , the coal seam stress is increased proportionally with the increase in uniform load  $\gamma h$ . (4) There is a significant stress concentration on the

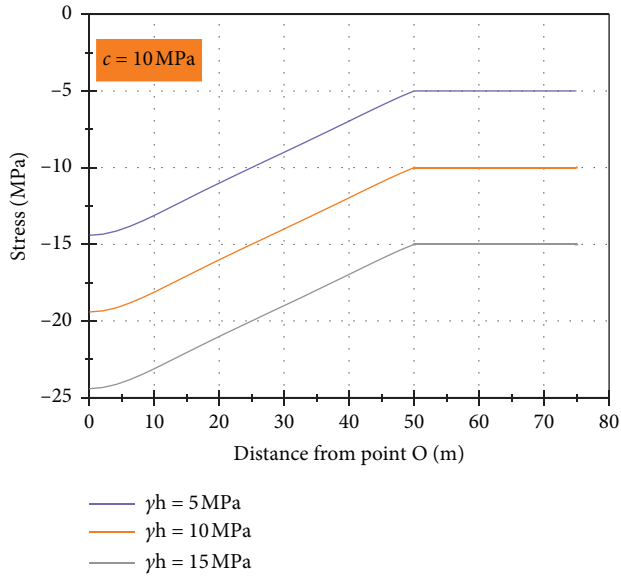


FIGURE 3: Change curves of nominal stress in a different uniform load  $\gamma h$ .

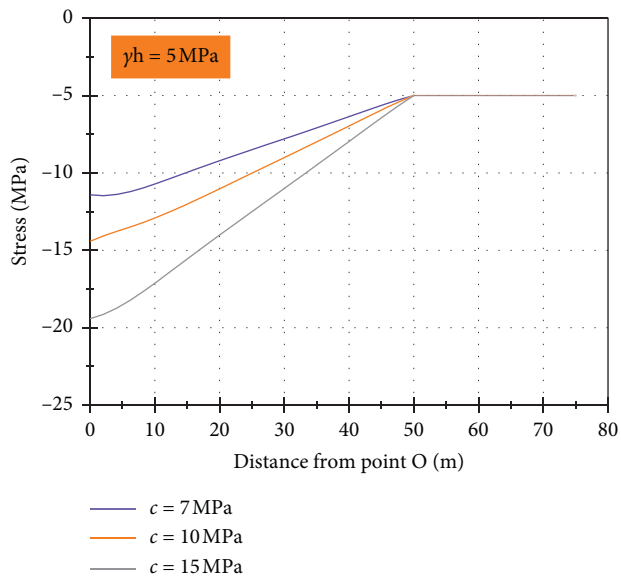


FIGURE 4: Change curves of nominal stress in a different parameter  $c$ .

origin position (the position of point O in Figure 2). And the farther away the point is, the lower the stress concentration is. The stress concentration continues to the edge of the mountain impact.

To further represent and verify the above phenomenon between stress and burial depth of the coal seam, the numerical modeling technology based on Flac<sup>3D</sup> was used in the Mechanical Model section. Compared to the previous study, two mountain peaks with heights of 60 m and 35 m to rock mass stress were considered in this model. The length, width, and height of this model were set as 200 m, 80 m, and 260 m, respectively. The dip angle of rock mass was 23° according to geological conditions in the Shabatai coal mine where the mechanical parameters used

in calculation were picked up. The applied parameters are listed in Table 1. Moreover, different boundary conditions were conducted to the model. The upper part of the model was free boundary, and the front, back, left, and right were horizontal displacement constraints. The vertical displacement restriction was applied on the bottom. Besides, the Mohr–Coulomb theory was used to calculate the model. A simulating result describing the SZZ contour map is shown in Figure 5.

The SZZ stress contour map obtained by numerical analysis and above studies exhibits good consistency in terms of the trend. It can be observed that the SZZ stress shows noteworthy nonlinear characteristics with change of burial depth. The SZZ stress under the peak is the largest, while it gets the smallest value at the edge. Compared to the higher peak, the value of SZZ stress under the lower peak is relatively small at a certain burial depth.

Although the results obtained through numerical simulation are slightly different from the above theoretical analysis, the results can still reflect the major mechanical behaviors of the relationship between burial depth and stress. Therefore, the numerical simulation and theoretical analysis are verified by each other.

**3.2. Permeability Change Laws of the Coal Seam on Mountainous Region Condition.** Based on equations (9), (11), and (15), parameters  $EI$ ,  $K$ , and  $l$  were selected according to Section 3.1. The porosity  $\phi_0$  was given the value of 1.5%, the initial gas pressure  $p_0$  was 1 MPa, and the pore compressibility  $c_\phi$  was  $0.5 \times 10^{-3} \text{ MPa}^{-1}$ . Let  $\gamma h = 5 \text{ MPa}$ ,  $p = 3 \text{ MPa}$ , and  $c = 7, 10, \text{ and } 15 \text{ MPa}$ . Change curves of the value of  $k/u$  in a different parameter  $c$  are shown in Figure 6.

(1) The permeability of the coal seam and the change in trend of nominal stress showed a good correlation, and with the increase in nominal stress, the permeability decreased significantly. (2) The larger the value of parameter  $c$ , the smaller the permeability of the coal seam under the same distance from the original point and then the greater the difficulty of gas flows and release. (3) The permeability at the original point reached the minimum value, and with the distance increasing from the point, the permeability increased gradually.

In view of the control effect of coal permeability on gas flow, the synergistic relationship between permeability and stress/strain of coal, the positive correlation between permeability and burial depth, the positive correlation between burial depth and gas content, and the positive correlation between permeability and gas content, many scholars have done a lot of research by means of laboratory tests and have obtained a series of beneficial results.

In this paper, the stress characteristics and permeability of the mountain pressurised by the coal seam were studied by means of mechanical analysis. The results showed that the burial depth, stress, and permeability of the coal seam pressurised by the overlying mountain have changed significantly, which can inevitably lead to the change of gas content. As our theoretical support, the similar results had been obtained in [2] and [3] by different study methods.

TABLE 1: Calculation parameters.

	Bulk modulus (GPa)	Shear modulus (GPa)	Internal friction angle (°)	Cohesion (MPa)	Tensile strength (MPa)	Density ( $\text{g}\cdot\text{cm}^{-3}$ )
Sandy mudstone	8	2	24	2.45	1.14	2.51
Fine sandstone	11	9.2	26	2.5	2.4	2.7
Mudstone	6.64	4.18	28	1.95	1.9	2.5
Coal seam	2.9	1.65	20	1.2	0.9	1.48
Coarse sandstone	12	10.8	31	2.9	2.3	2.65
Medium sandstone	11	8	25	3.3	2.2	2.75

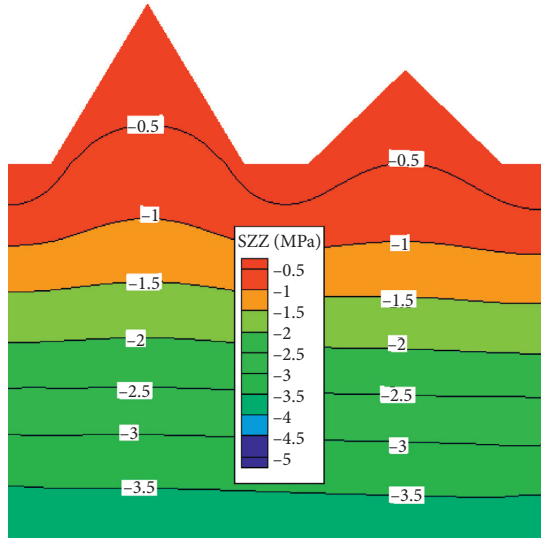
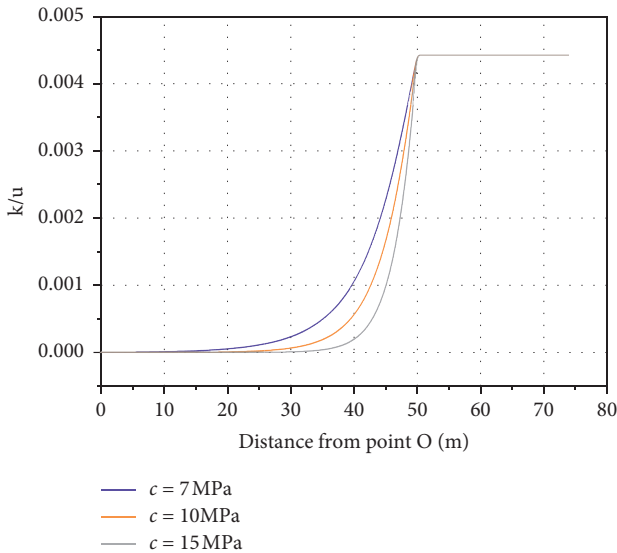


FIGURE 5: Distribution of SZZ.

FIGURE 6: Change curves of the value of  $k/u$  in different  $c$ .

#### 4. Gas Enrichment Laws of the Coal Seam on Mountainous Region Condition

We have obtained the gas enrichment mechanism influenced by vertical stress on mountainous region condition by the aforementioned study. It is well known that the gas

emission rate and gas content are characteristic parameters to express gas enrichment which was mainly affected by stress and permeability.

##### 4.1. Gas Emission Rate Changing Laws during Tunneling

**4.1.1. Project Background.** The Shabatai coal mine is a high gas mine in the Ningxia Hui Autonomous Region, China. The coal seam is deposited beneath to the Helan Mountains. The surface elevation is +1440 m~+1670 m, with the maximum relative height difference of 230 m.

The strike longwall retreating mining method is adapted in the 10502 working face. The strike length of the working face is 950 m, with the width of 210 m. And the dip length of it is 210 m, with the dip angle of 23°. Given the influence by mountains, the surface elevation of the mountain above the ventilation roadway in the 10502 working face is from 1540 m to 1610 m, resulting in the burial depth of 300~370 m. This dramatic difference in burial depth might lead to a great change in the gas emission rate and gas content. The surface elevation changing characteristics above the ventilation roadway in the 10502 working face is shown in Figure 7.

**4.1.2. Gas Emission Rate during the Ventilation Roadway Tunneling.** For accurately studying the absolute gas emission rate on condition, the coal-bed methane was not the adopted measures of premining drainage before tunneling. No fold, fault, and other geological structures were found during tunneling, which excluded the influence of the geological structure on gas emission. In order to minimize the impact of driving speed on gas emission, we adopted a smaller excavation speed, namely, 2-3 m per day. The absolute gas emission rate is shown in Figure 8.

It can be divided into four regions according to surface elevation. We can see that there are great disparities in the gas emission rate for different regions. And the gas emission rate during tunneling corresponds to the changes of surface elevation. (1) Specifically, the absolute gas emission rate shows an increasing trend in region 1# with surface elevation increasing from 1540 m to 1550 m. (2) The growth trend of absolute gas emission is obvious mild in region 2# when the surface elevation increases from 1550 m to 1610 m slowly. (3) The absolute gas emission rate keeps oscillating at high values in region 3# when surface elevation is kept at 1610 m. (4) Thereafter, as the surface elevation drops rapidly from 1610 m to 1556 m in region 4#, the absolute gas emission rate

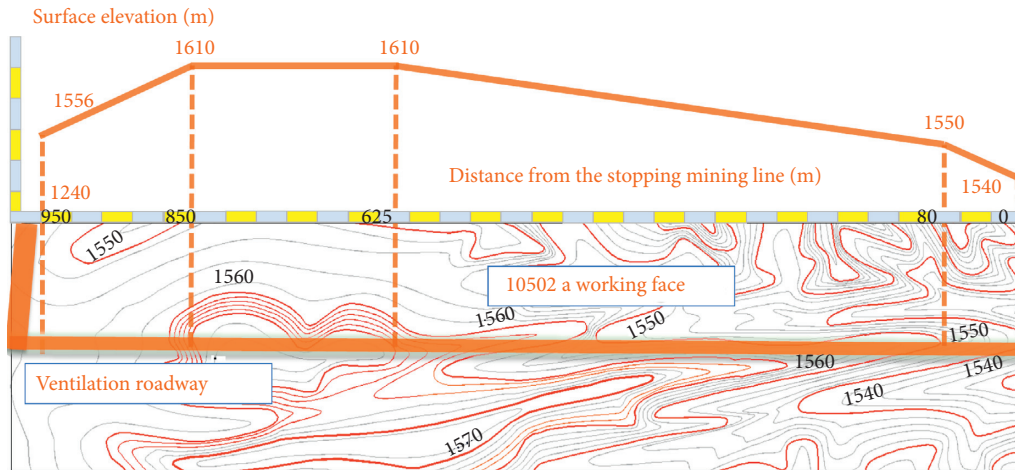


FIGURE 7: Surface elevation changing characteristics above the ventilation roadway in the 10502 working face.

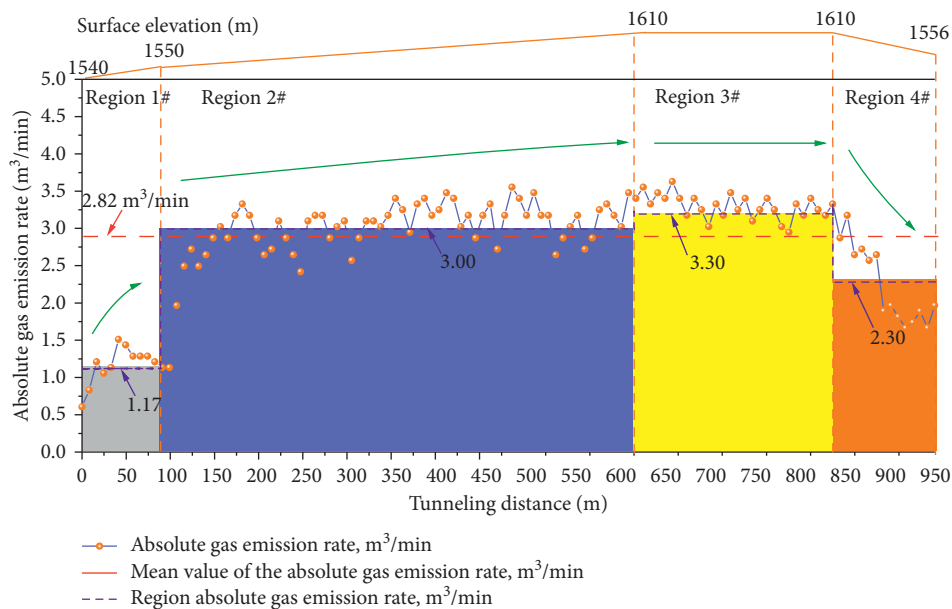


FIGURE 8: Curve of the absolute gas emission rate of the ventilation roadway in the 10502 working face during tunneling.

significantly decreases accordingly. Also, the similar trend appears in the mean value of the gas emission rate at different regions. The quantities of that are 1.17 m<sup>3</sup>/min, 3.00 m<sup>3</sup>/min, 3.30 m<sup>3</sup>/min, and 2.30 m<sup>3</sup>/min, respectively, from regions 1# to 4#.

#### 4.2. Determining of Coal Seam Gas Content near the Ventilation Roadway

4.2.1. Method. DGC is the most popular gas content measuring device in China. It is developed and manufactured by the China Coal Technology Engineering Group Chongqing Research Institute. The Government has issued the national standard “direct measurement method of coal seam gas content in mines” (GB/T23250-2009) in 2009 based on it. The

device consists of 7 parts: the underground coring and desorption system, ground gas desorption system, weighing system, coal sample crushing system, moisture measurement system, gas composition measurement system, and data processing system. The method has the advantages of short determination period, low cost, small laboratory workload, and higher success rate. Particularly, the gas content determination work can be completed within 8 hours. The device is shown in Figure 9, and the measuring process is shown in Figure 10.

The borehole for the determination of gas content was set perpendicular to the ventilation roadway, one every 50 meters. The samplings were all taken at 70 m depth. And, 19 holes were set in the roadway in total. The sketch map of gas content measurement drilling in the ventilation roadway is shown in Figure 11. The determination results of gas content of the coal seam are shown in Figure 12.



FIGURE 9: Direct measuring device for gas content.

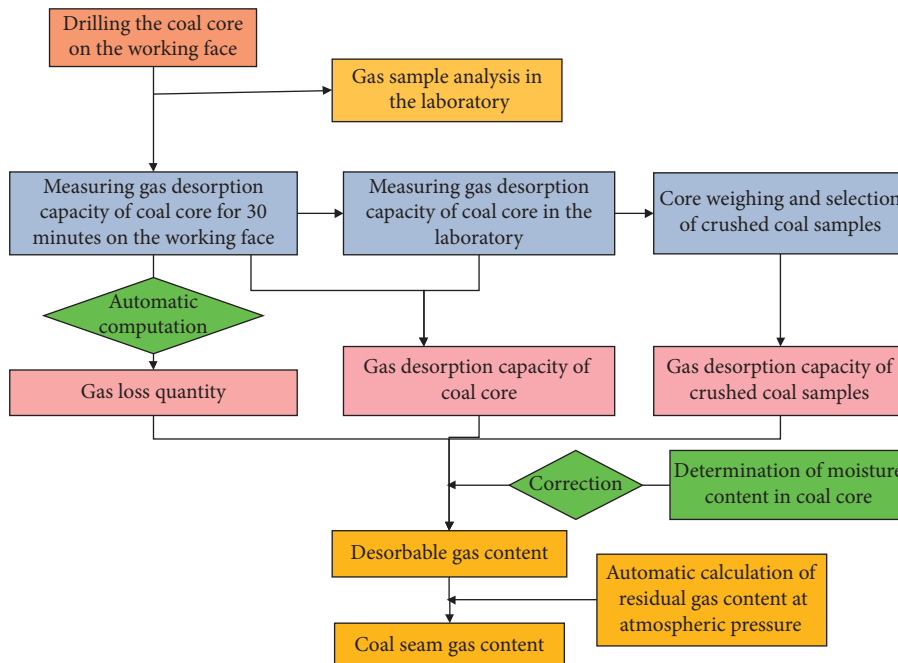


FIGURE 10: Gas content determination process.

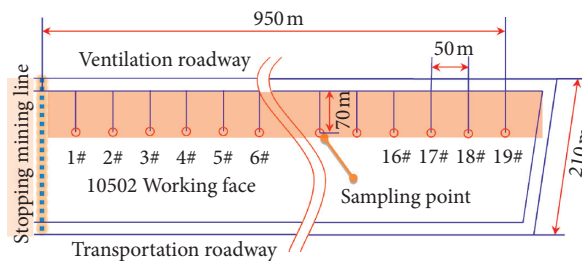


FIGURE 11: Sketch map of gas content measurement drilling in the ventilation roadway.

4.2.2. Results. It can be seen that the gas content can be generally divided into four regions according to changing of surface elevation. At region 1#, gas content presents a prominent uptrend with the rise of the surface elevation.

While, at region 2#, the changes of gas content maintain a certain balance and fluctuate around the mean. For region 3#, the value of gas content implies a degree of increase with the surface elevation rising from 1550 m to 1558 m.



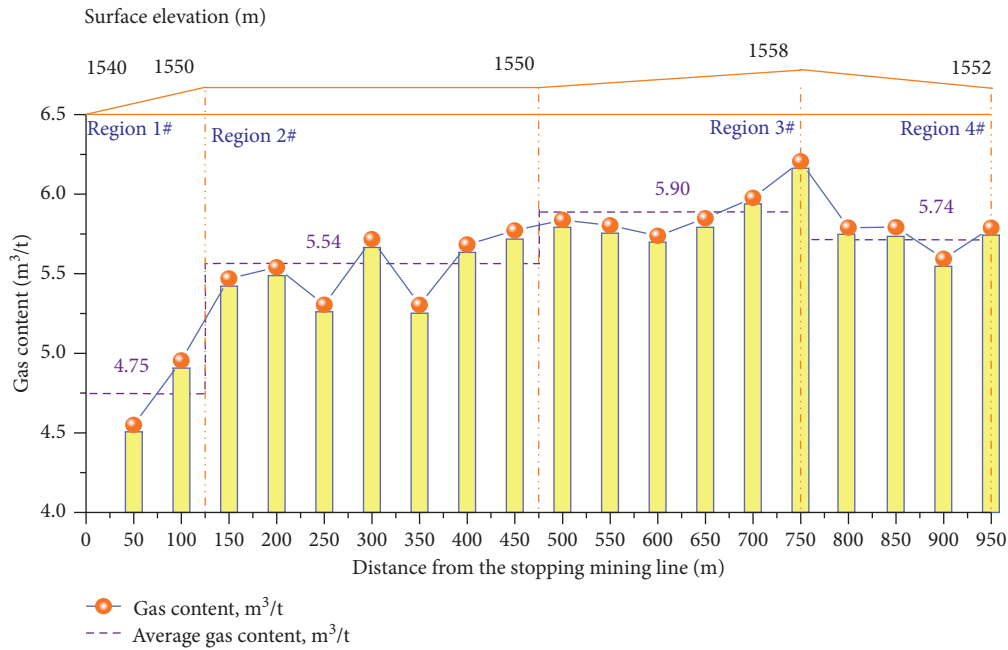


FIGURE 12: Determination results of gas content along the ventilation roadway.

Particularly, gas content at region 4# shows a significant decline as the drop of surface elevation.

Thus, Figure 12 reveals that there has been a sharp correlation between methane content of the coal seam and changes of surface elevation under mountainous condition. The similar conclusion can be obtained for the changing trends of the mean gas content of the four regions. The values of those are  $4.75 \text{ m}^3/\text{t}$ ,  $5.54 \text{ m}^3/\text{t}$ ,  $5.90 \text{ m}^3/\text{t}$ , and  $5.74 \text{ m}^3/\text{t}$ , respectively.

## 5. Conclusion

Gas occurrence of coal seam is closely related to the overlying mountain, which has always been ignored. Based on the Winkler elastic foundation beam theory, seepage theory, and the method of field observation, the change rules of stress and permeability of the coal seam pressurised by the overlying mountain were studied. Then, the relationship between burial depth, stress, permeability, and gas content was analyzed. As a result, the gas enrichment mechanism of the coal seam pressurised by the overlying mountain was studied:

- (1) The mechanical model of the coal seam pressurised by the overlying mountain was established and analyzed based on the Winkler elastic foundation beam theory and seepage theory. The theoretical solution to nominal stress was derived. Then, the theoretical solution to permeability with nominal stress and gas pressure as variables was obtained.
- (2) The change rules of stress and permeability of the coal seam pressurised by the overlying mountain were studied based on the method of example analysis. The results showed that the changes of the stress and permeability are significantly consistent

with the changes of burial depth and surface elevation.

- (3) It shows a strong correlation between surface elevation, depth, stress, and permeability on the condition of the coal seam pressurised by the overlying mountain. The initial gas content is controlled by the permeability and the stress of the coal seam. Also, the field practice showed that there was a significant positive correlation between the initial gas content, surface elevation, and burial depth. At the same time, the absolute gas emission rate during roadway driving showed the same characteristics.
- (4) This new finding is helpful to understand the essential mechanism of the increase of coal-bed methane occurrence under mountainous area condition and gives the implication of solving the gas disaster. Under this condition, we can take measures such as increasing the density of the gas drainage borehole and extracting time so as to further reduce the gas disaster and obtain coal-bed methane resources as much as possible.

## Data Availability

The data supporting the findings of this study are included within the article and its supplementary materials.

## Conflicts of Interest

The authors declare no conflicts of interest.

## Authors' Contributions

X. Y. conceived the theme; R. H. carried out the theoretical derivation; R. H., J. L., and F. Z. designed and performed the

field tests; B. C., S. S., and C. H. provided theoretical and technical guidance; R. H. analyzed the data and wrote the paper.

## Acknowledgments

This research was funded by the Fundamental Research Funds for the Central Universities (Grant no. 2020YJSSB03) and the National Nature Science Foundation of China (Grant no. 41672347).

## References

- [1] K. Bandyopadhyay, J. Mallik, R. Shajahan, and N. Agarwal, "Closing the gap between analytical and measured coal permeability," *Fuel*, vol. 281, 2020.
- [2] J. Lu, G. Yin, B. Deng et al., "Permeability characteristics of layered composite coal-rock under true triaxial stress conditions," *Journal of Natural Gas Science and Engineering*, vol. 66, pp. 60–76, 2019.
- [3] M. Kudasik, "Investigating permeability of coal samples of various porosities under stress conditions," *Energies*, vol. 12, no. 4, p. 762, 2019.
- [4] G. R. Wang, D. J. Xue, and H. L. Gao, "Study on permeability characteristics of coal rock in complete stress-strain process," *Journal of China Coal Society*, vol. 37, pp. 107–112, 2012.
- [5] S. P. Meng, B. Y. Wang, and X. T. Xie, "Mechanical properties of coal deformation and its influence on permeability," *Journal of China Coal Society*, vol. 37, pp. 1342–1347, 2012.
- [6] N. Cao, G. Lei, and P. C. Dong, "Stress-dependent permeability of fractures in tight reservoirs," *Energies*, vol. 12, p. 117, 2019.
- [7] Y. Song, B. Jiang, M. Li, C. L. Hou, and S. C. Xu, "A review on pore-fractures in tectonically deformed coals," *Fuel*, vol. 278, 2020.
- [8] H.-D. Chen, C. Yuan-Ping, H.-X. Zhou, and W. Li, "Damage and permeability development in coal during unloading," *Rock Mechanics and Rock Engineering*, vol. 46, no. 6, pp. 1377–1390, 2013.
- [9] C. Zhang and L. Zhang, "Permeability characteristics of broken coal and rock under cyclic loading and unloading," *Natural Resources Research*, vol. 28, no. 3, pp. 1055–1069, 2019.
- [10] Z. Fang, X. Li, and L. Huang, "Laboratory measurement and modelling of coal permeability with different gases adsorption," *International Journal of Oil, Gas and Coal Technology*, vol. 6, no. 5, pp. 567–580, 2013.
- [11] Z. Ye, L. Zhang, D. Hao, C. Zhang, and C. Wang, "Experimental study on the response characteristics of coal permeability to pore pressure under loading and unloading conditions," *Journal of Geophysics and Engineering*, vol. 14, no. 5, pp. 1020–1031, 2017.
- [12] K. Wang, F. Du, and X. Zhang, "Mechanical properties and permeability evolution in gas-bearing coal-rock combination body under triaxial conditions," *Environmental Earth Sciences*, vol. 76, p. 815, 2017.
- [13] Y. Gensterblum, A. Ghanizadeh, and B. M. Krooss, "Gas permeability measurements on Australian subbituminous coals: fluid dynamic and poroelastic aspects," *Journal of Natural Gas Science and Engineering*, vol. 19, pp. 202–214, 2014.
- [14] P. F. Ren, D. Z. Tang, and H. Xu, "Control mechanism of buried depth and in-situ stress for coal reservoir permeability in liulin area," *Bulletin of Science and Technology*, vol. 32, pp. 25–29, 2016.
- [15] M. Zhang, X. Fu, and H. Wang, "Analysis of physical properties and influencing factors of middle-rank coal reservoirs in China," *Journal of Natural Gas Science and Engineering*, vol. 50, pp. 351–363, 2018.
- [16] M. Li, B. Jiang, S. Lin, F. Lan, and G. Zhang, "Characteristics of coalbed methane reservoirs in faer coalfield, western guizhou," *Energy Exploration & Exploitation*, vol. 31, no. 3, pp. 411–428, 2013.
- [17] H. Z. Zhou, P. Liu, and P. Chen, "Analysis of coalbed methane occurrence in Shuicheng Coalfield, southwestern China," *Journal of Natural Gas Science & Engineering*, vol. 47, pp. 140–153, 2017.
- [18] Q. Li, "Simulation and verification of gas occurrence law in deep coal seams of dingji coal mine," *Safety in Coal Mines*, vol. 46, pp. 166–169, 2015.
- [19] J. Q. Kang, X. H. Fu, D. Elsworth, and S. Liang, "Vertical heterogeneity of permeability and gas content of ultra-high-thickness coalbed methane reservoirs in the southern margin of the Junggar Basin and its influence on gas production," *Journal of Natural Gas Science & Engineering*, vol. 81, 2020.
- [20] G. Z. Yin, W. P. Li, and M. H. Li, "Permeability properties and effective stress of raw coal under loading-unloading conditions," *Journal of China Coal Society*, vol. 39, pp. 1497–1503, 2014.
- [21] X. Y. Li, N. J. Ma, and Y. P. Zhong, "Storage and release regularity of elastic energy distribution in tight roof fracturing," *Chinese Journal of Rock Mechanics and Engineering*, vol. 26, pp. 2786–2793, 2007.
- [22] X. Z. Xu, P. C. Li, and C. L. Li, "Study on the principle of effective stress in porous media," *Mechanics in Engineering*, vol. 23, pp. 42–45, 2001.
- [23] Y. Huang and F. S. He, *Beams, Plates and Shells on Elastic Foundation*, pp. 26–28, Science Press, Beijing, China, 1st edition, 2005.
- [24] F. Hou, *The analytical solution of the winkler beam under the uniform distributed load and its application in the longitudinal calculation of the shield tunnel*, Ph.D. Thesis, Qingdao Technological University, Qingdao, China, 2009.